Formation of Li^+ superionic crystals from the Li_2S–P_2S_5 melt-quenched glasses

**Akitoshi Hayashi · Keiichi Minami ·
Fuminori Mizuno · Masahiro Tatsumisago**

Abstract The $70Li_2S\cdot30P_2S_5$ (mol%) glass was prepared by the melt quenching method and the glass–ceramic electrolytes were obtained by heating the prepared glass over crystallization temperatures. The superionic metastable $Li_7P_3S_{11}$ crystal was formed by heating the glass in the temperature range from 280 and 360 °C. The conductivity of the glass–ceramics was enhanced by the precipitation and growth of the $Li_7P_3S_{11}$ crystal, and the highest conductivity of 4.1×10^{-3} S cm^{-1} at room temperature was achieved in the glass–ceramic heated at 360 °C for 1 h. The $Li_7P_3S_{11}$ crystal changed into the thermodynamically stable phase such as the $Li_4P_2S_6$ crystal with further increasing heat treatment temperature and holding time, resulting in lowering conductivities of the glass–ceramics.

Introduction

Li_2S-based sulfide glassy materials are known to show high Li^+ conductivity [1, 2] and then these glasses are promising candidates for solid electrolytes of all-solid-state lithium batteries with high safety and reliability. Much effort has been devoted to the improvement of Li^+ conductivity for sulfide-based glassy solid electrolytes [3]. Although the crystallization of glassy ionic conductors generally decreases conductivity, we found that the conductivity was enhanced by the crystallization of the Li_2S–P_2S_5 glasses [4–6]. In particular, a superionic $Li_7P_3S_{11}$ crystal was

A. Hayashi (✉) · K. Minami · F. Mizuno · M. Tatsumisago
Department of Applied Chemistry, Graduate School
of Engineering, Osaka Prefecture University, 1-1 Gakuen-cho,
Naka-ku, Sakai, Osaka 599-8531, Japan
e-mail: hayashi@chem.osakafu-u.ac.jp

precipitated at the composition of 70 mol% Li_2S; the obtained glass–ceramic electrolyte exhibited the highest conductivity of 3.2×10^{-3} S cm^{-1} at 25 °C in all the Li^+ ion conductors ever known [6]. The mother sulfide glasses were synthesized by a mechanochemical technique using a planetary ball mill apparatus. A lot of sulfide-based glassy and glass–ceramic solid electrolytes were successfully prepared by mechanical milling [3–9], and all-solid-state cells using these solid electrolytes worked as lithium secondary batteries with high specific capacity and excellent cycling performance [10].

Recently, we have prepared the $70Li_2S\cdot30P_2S_5$ (mol%) glasses by a melt quenching technique with various melting conditions, and local structure and electrical properties of the glasses were investigated [11]. It was revealed that the glasses were mainly composed of $P_2S_7^{4-}$ and PS_4^{3-} ions and the local structure of the glasses was affected by the melting temperature; the $P_2S_6^{4-}$ ions tended to form instead of $P_2S_7^{4-}$ ions with increasing melting temperatures from 750 to 900 °C. The local structure of the glass prepared by quenching the melt, which was heated at 750 °C for 20 h, was similar to that prepared by mechanical milling. The $Li_7P_3S_{11}$ crystal was precipitated by crystallization of the quenched glasses as well as the milled glasses, and the presence of the crystal enhanced the conductivity of the glass–ceramic electrolytes. Crystalline phases precipitated from the $70Li_2S\cdot30P_2S_5$ milled glass changed with heating temperature, and the conductivity of glass–ceramics depended on the crystalline phases; superionic $Li_7P_3S_{11}$ was formed at heating temperatures of 240 and 360 °C, while less conductive $Li_4P_2S_6$ was crystallized at 550 °C [6]. The formation process of the $Li_7P_3S_{11}$ from the quenched glasses has not been clarified and it is important to develop the glass–ceramic electrolytes with higher conductivity.

In the present study, the crystallization process of the Li_2S–P_2S_5 glasses prepared by melt quenching was examined. The glass–ceramic materials were prepared and optimized by heating the glasses at various temperatures above the crystallization temperature and holding them for several hours. Local structure of the glass–ceramics was investigated by Raman spectroscopy and the precipitated crystals were identified by XRD measurements. The relationship between the crystals precipitated in the glass–ceramics and their conductivities will be discussed.

Experimental

Reagent-grade Li_2S (Idemitsu Kosan, 99.9%) and P_2S_5 (Aldrich, 99%) crystalline powders were used as starting materials to prepare the glass at the composition $70Li_2S\cdot30P_2S_5$ (mol%). The mixture of these crystals was put into a carbon coated quartz tube in a dry Ar-filled grove box and then the tube was sealed under vacuum. The quartz tube was heated at 750 °C for 10 h, and the glasses were prepared by quenching of molten samples with ice water.

Differential thermal analysis (DTA) was carried out using a thermal analyzer (Rigaku, Thermo-plus 8110) for the glassy powders sealed in an Al pan in a dry N_2 atmosphere; the heating rate was 10 °C min^{-1}. Raman spectra of the glasses were measured with a Raman spectrophotometer (JASCO, NR-1000) using the 514 nm line of an Ar^+ laser beam. X-ray diffraction (XRD) measurements (Cu Kα) were performed using a diffractometer (Bruker AXS, M18XHF[22]-SRA) to identify crystalline phases precipitated in the glass–ceramic materials. Electrical conductivities were measured for the pelletized glassy and glass–ceramic samples with 10 mm in diameter and about 1 mm in thickness. A carbon paste was painted onto both sides of a sample and carbon electrodes were formed after heat treatment. AC impedance measurements were carried out in dry Ar atmosphere using an impedance analyzer (Solartron, SI1260) in the frequency range of 10 Hz to 8 MHz. The temperature range of the measurements was from 25 to 280 °C.

Results and discussion

Figure 1 shows the DTA curve of the $70Li_2S\cdot30P_2S_5$ (mol%) glass prepared by the melt quenching method. An endothermic change due to glass transition at around 230 °C and two sharp exothermic peaks due to crystallization at around 270 and 430 °C are observed. The glass–ceramic samples were prepared by heating the glass at several temperatures over the crystallization temperatures in order to examine local structure and precipitated crystal phases of the glass–ceramics.
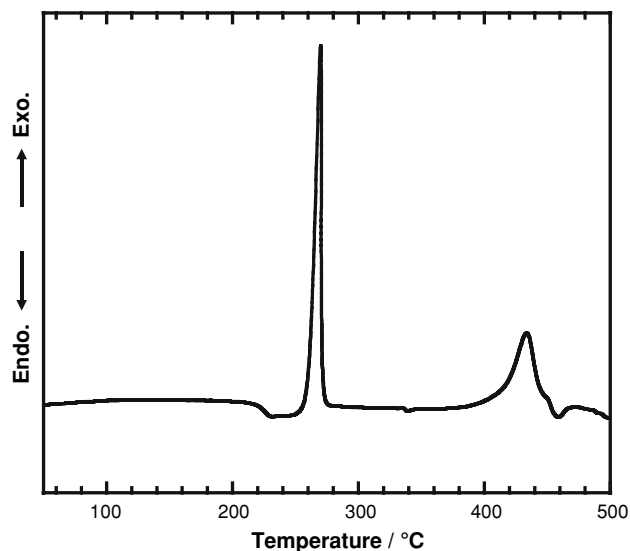
Fig. 1 DTA curve of the $70Li_2S\cdot30P_2S_5$ glass prepared by the melt quenching method

Figure 2 shows the Raman spectra of the $70Li_2S\cdot30P_2S_5$ (mol%) glass and glass–ceramics prepared by heat treatment of the glass at several temperatures 280, 360, and 450 °C. Two peaks at 406 and 419 cm^{-1} are observed in the spectra of the glass and glass–ceramics heated at 280 and 360 °C. The intense peak at 382 cm^{-1} and the weak peak at 419 cm^{-1} are observed in the spectrum of the
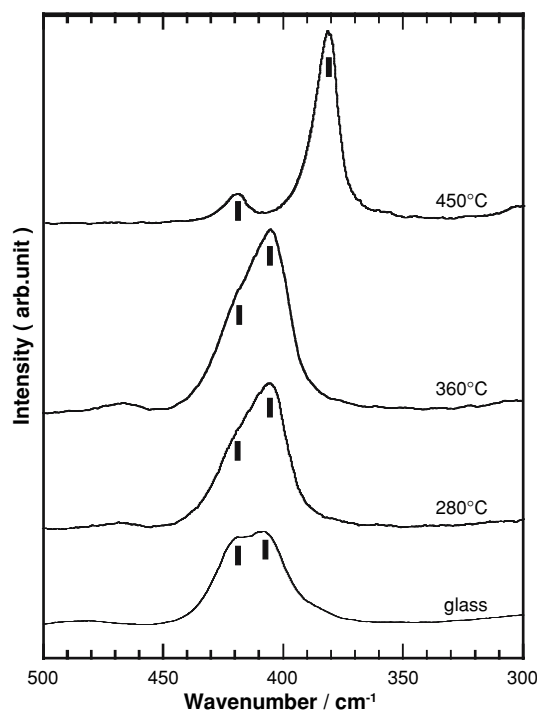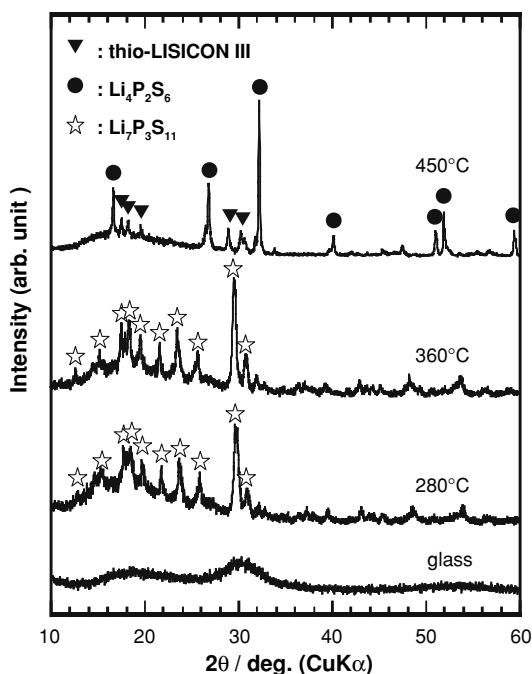

Fig. 2 Raman spectra of the $70Li_2S\cdot30P_2S_5$ (mol%) glass and glass–ceramics prepared by heat treatment of the glass at several temperatures, 280, 360, and 450 °C

glass–ceramic heated at 450 °C. The peaks at 382, 406, and 419 cm^{-1} are attributable to the $P_2S_6^{4-}$, $P_2S_7^{4-}$, and PS_4^{3-} ions, respectively [12]. The 70Li$_2$S·30P$_2$S$_5$ glass is composed of the $P_2S_7^{4-}$ and PS_4^{3-} ions, and the local structure of the glass is similar to that of the glass prepared by mechanical milling [11]. The glass–ceramics prepared by heat treatment over the first crystallization temperature (ca. 260 °C) consist of the $P_2S_7^{4-}$ and PS_4^{3-} ions, which are also observed in the glass. On the other hand, large structural change occurs over the second crystallization temperature (ca. 400 °C) and the glass–ceramic prepared at 450 °C is composed of the $P_2S_6^{4-}$ and PS_4^{3-} ions and the $P_2S_7^{4-}$ ions are no longer present.
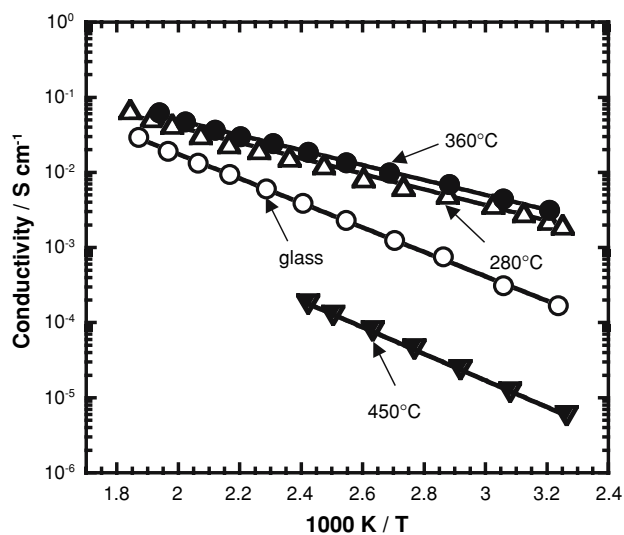
Figure 3 shows the XRD patterns of the 70Li$_2$S·30P$_2$S$_5$ glass–ceramics prepared by heat treatment at several temperatures 280, 360, and 450 °C. The patterns of glass–ceramics prepared at 280 and 360 °C are attributable to the superionic Li$_7$P$_3$S$_{11}$ crystal. The crystal is firstly prepared by the crystallization of the 70Li$_2$S·30P$_2$S$_5$ mechanically milled glass, and could not be prepared by conventional solid-state reaction [5]. The crystal structure of Li$_7$P$_3$S$_{11}$ has just been clarified [13] and the crystal is composed of the $P_2S_7^{4-}$ and PS_4^{3-} ions. On the other hand, the Li$_4$P$_2$S$_6$ crystal is mainly present and the crystal analogous to the thio-LISICON III phase in the Li$_4$GeS$_4$–Li$_3$PS$_4$ solid solution [14] is also observed in the glass–ceramic prepared at 450 °C, which is just above the second crystallization peak temperature in Fig. 1. The Li$_7$P$_3$S$_{11}$ phase changes into the thermodynamically stable crystalline phases such as

Li$_4$P$_2$S$_6$ at 450 °C, indicating that Li$_7$P$_3$S$_{11}$ is a metastable phase. The Raman spectra of the glass–ceramics as shown in Fig. 2 correspond to the crystalline phases identified by XRD measurements. The crystallization of the mechanically milled 70Li$_2$S·30P$_2$S$_5$ glass was examined and the first precipitated crystals was Li$_7$P$_3$S$_{11}$ and then Li$_4$P$_2$S$_6$ and thio-LISICON III analog were formed with increasing heat treatment temperature [6]. It is revealed that the crystallization process of the 70Li$_2$S·30P$_2$S$_5$ melt-quenched glass is similar to that of the milled glass.

Figure 4 shows the temperature dependence of electrical conductivity for the pelletized samples of the 70Li$_2$S·30P$_2$S$_5$ glass and glass–ceramics. The glass–ceramic samples were prepared by heating the glass up to the targeted temperatures 280, 360, and 450 °C and then cooling down to room temperature. The conductivities of all the samples obey the Arrhenius equation. The conductivity of the glass is increased by increasing heat treatment temperature up to 360 °C; the glass–ceramic heated at 360 °C exhibits the ambient temperature conductivity of 2.3×10^{-3} S cm^{-1}, which is one order of magnitude higher than the conductivity of the glass. On the other hand, the glass–ceramic heated at 450 °C shows lower conductivity of 3.8×10^{-6} S cm^{-1} at room temperature. The heating temperature dependence of activation energy for conduction corresponds to that of conductivity at room temperature, and the lowest activation energy of 18 kJ mol^{-1} is obtained for the glass–ceramic prepared by heat treatment at 360 °C. It was revealed that electronic conductivity was negligible and lithium ion transport number was almost unity for the glass–ceramics prepared from melt-quenched 70Li$_2$S·30P$_2$S$_5$ glasses [11].

Fig. 3 XRD patterns of the 70Li$_2$S·30P$_2$S$_5$ glass and glass–ceramics prepared by heat treatment at several temperatures, 280, 360, and 450 °C

Fig. 4 Temperature dependence of electrical conductivity for the pelletized samples of the 70Li$_2$S·30P$_2$S$_5$ glass and glass–ceramics prepared by heat treatment at several temperatures 280, 360, and 450 °C

The relationship between the crystalline phases in the glass–ceramics and their conductivities is discussed. In the glass–ceramics heated at 280 and 360 °C, the highly conductive $Li_7P_3S_{11}$ crystal was formed. The highest conductivity obtained by heat treatment at 360 °C would be caused by both the precipitation and the increase in crystallinity of the $Li_7P_3S_{11}$ crystal. On the other hand, the $Li_4P_2S_6$ crystal was mainly formed in the glass–ceramic heated at 450 °C. Since lithium ion conductivities of the $Li_4P_2S_6$ crystal are lower than 10^{-7} S cm^{-1} at room temperature [12], the glass–ceramic heated at 450 °C exhibited low conductivity. It is obvious that the conductivities of the Li_2S–P_2S_5 glass–ceramics largely depend on the precipitated crystalline phases. Although lithium ion conduction mechanism of $Li_7P_3S_{11}$ has not been clarified, the precipitation of $Li_7P_3S_{11}$ is closely related to the high conductivity and low activation energy for conduction of the Li_2S–P_2S_5 glass–ceramics.

Improvement in crystallinity of the metastable $Li_7P_3S_{11}$ crystal is a key point for further enhancement of the conductivity of the glass–ceramics. The glass–ceramics were then prepared by holding the glass at 360 °C for longer periods of time in order to form $Li_7P_3S_{11}$ with higher crystallinity. Figure 5 shows the temperature dependence of electrical conductivity for the pelletized samples of the $70Li_2S\cdot30P_2S_5$ glass–ceramics, which were prepared by heating the glass at 360 °C for the different holding times of 0, 1, 2, and 5 h. The conductivity of the glass–ceramics at room temperature increases by increasing the holding time up to 1 h. The highest conductivity of 4.1×10^{-3} S cm^{-1} at room temperature and the lowest activation energy of
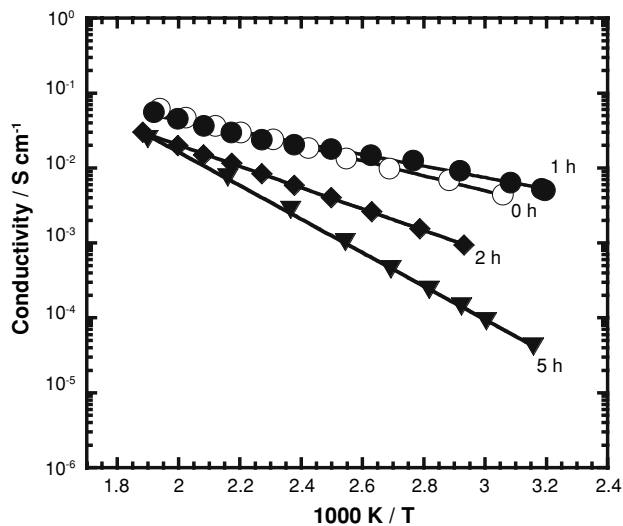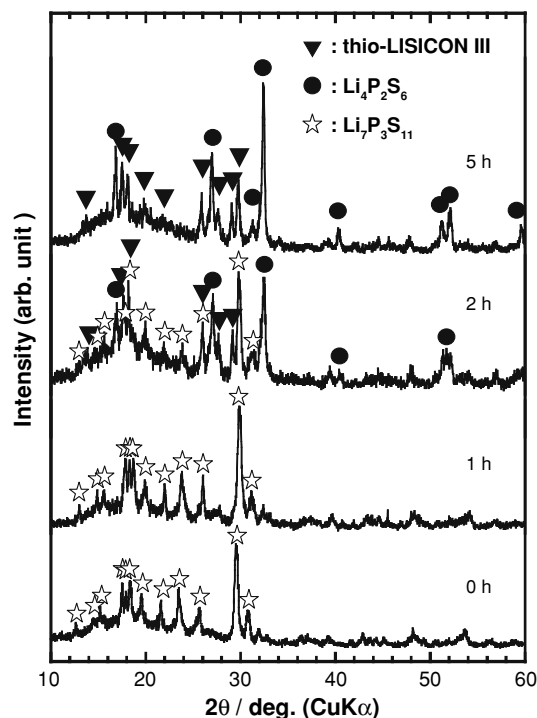
14 kJ mol^{-1} for conduction are obtained for the glass–ceramic prepared by heating the glass at 360 °C for 1 h. Taking the longer holding times over 1 h, however, decreases the conductivity of the glass–ceramics. The ambient temperature conductivities of the glass–ceramics heated for 2 and 5 h are 3.1×10^{-4} and 1.7×10^{-5} S cm^{-1}, respectively. The highest activation energy of 42 kJ mol^{-1} is obtained for the glass–ceramic heated for 5 h.

Figure 6 shows the XRD patterns of the $70Li_2S\cdot30P_2S_5$ glass–ceramics prepared by heating the glass at 360 °C for several hours. The intensity of the XRD peaks due to $Li_7P_3S_{11}$ increases with increasing the holding time up to 1 hour. The XRD patterns due to the $Li_4P_2S_6$ crystal and the thio-LISICON III analog as well as $Li_7P_3S_{11}$ are observed in the glass–ceramic heated for 2 h. The XRD peaks due to $Li_7P_3S_{11}$ completely vanish and the intensity of the peaks due to $Li_4P_2S_6$ and the thio-LISICON III analog increases by a further increase in the holding time up to 5 h. The improvement of the crystallinity of $Li_7P_3S_{11}$ brings about the highest conductivity for the glass–ceramic heated at 360 °C for 1 h. On the other hand, the conductivity decreased and activation energy for conduction increased with increasing the holding time over 1 h because of the precipitation of $Li_4P_2S_6$ with low conductivity.

The glass–ceramic solid electrolyte with the high conductivity of 4.1×10^{-3} S cm^{-1} at room temperature was successfully prepared by controlling heating temperature

Fig. 5 Temperature dependence of electrical conductivity for the pelletized samples of the $70Li_2S\cdot30P_2S_5$ glass–ceramics, which were prepared by heating the glass at 360 °C for the different holding times of 0, 1, 2, and 5 h

Fig. 6 XRD patterns of the $70Li_2S\cdot30P_2S_5$ glass–ceramics prepared by heating the glass at 360 °C for several hours

and holding time for the $70Li_2S\cdot30P_2S_5$ melt-quenched glass.

Conclusions

The $70Li_2S\cdot30P_2S_5$ glass was prepared by the melt quenching method and the glass–ceramic electrolytes were obtained by heating the prepared glass above crystallization temperatures. The highly conductive $Li_7P_3S_{11}$ crystal was formed by heating the glass in the temperature range from 280 to 360 °C. The conductivity of the glass–ceramics was enhanced by the precipitation and growth of the $Li_7P_3S_{11}$ crystal, and the highest conductivity of 4.1×10^{-3} S cm^{-1} at room temperature and activation energy of 14 kJ mol^{-1} for conduction were achieved in the glass–ceramic heated at 360 °C for 1 h. The $Li_7P_3S_{11}$ crystal changed into the thermodynamically stable phase of the $Li_4P_2S_6$ crystal, with further increased heat treatment temperature and holding time, resulting in lowering conductivities of the glass–ceramics. The formation and crystal growth of superionic metastable $Li_7P_3S_{11}$ crystal is very important to attain high conductivities and low activation energies for conduction of the $Li_2S–P_2S_5$ glass–ceramics as a promising solid electrolyte for all-solid-state lithium secondary batteries.

References

1. Mercier R, Malugani JP, Fahys B (1981) Solid State Ionics 5:663
2. Pradel A, Ribes M (1986) Solid State Ionics 18/19:351
3. Tatsumisago M, Hayashi A (2005) Solid state ionics for batteries. Springer-Verlag, p 32
4. Hayashi A, Hama S, Minami T, Tatsumisago M (2003) Electrochem Commun 5:111
5. Mizuno F, Hayashi A, Tadanaga K, Tatsumisago M (2005) Adv Mater 17:918
6. Mizuno F, Hayashi A, Tadanaga K, Tatsumisago M (2005) Electrochem Solid-State Lett 8:A603
7. Morimoto H, Yamashita H, Tatsumisago M, Minami T (1999) J Am Ceram Soc 82:1352
8. Tatsumisago M, Yamashita H, Hayashi A, Morimoto H, Minami T (2000) J Non-Cryst Solids 274:30
9. Hayashi A, Fukuda T, Hama S, Yamashita H, Morimoto H, Minami T, Tatsumisago M (2004) J Ceram Soc Jpn 112:S695
10. Mizuno F, Hama S, Hayashi A, Tadanaga K, Minami T, Tatsumisago M (2002) Chem Lett 1244
11. Minami K, Mizuno F, Hayashi A, Tatsumisago M (2007) Solid State Ionics 178:837
12. Tachez M, Malugani JP, Mercier R, Robert G (1984) Solid State Ionics 14:181
13. Yamane H, Shibata M, Shimane Y, Junke T, Seino Y, Adams S, Minami K, Hayashi A, Tatsumisago M (2007) Solid State Ionics 178:1163
14. Kanno R, Murayama M (2001) J Electrochem Soc 148:A742